

Contribution to assessing the stiffness reduction of structural elements in the global stability analysis of precast concrete multi-storey buildings

Contribuição para a avaliação da redução da rigidez de elementos estruturais de concreto pré-moldado de edifícios de múltiplos pavimentos para análise da estabilidade global



M. C. MARIN ^a
cuadradomarin@yahoo.com.br

M. K. EL DEBS ^b
mkdebs@sc.usp.br

Abstract

This study deals with the reduction of the stiffness in precast concrete structural elements of multi-storey buildings to analyze global stability. Having reviewed the technical literature, this paper presents indications of stiffness reduction in different codes, standards, and recommendations and compares these to the values found in the present study. The structural model analyzed in this study was constructed with finite elements using ANSYS® software. Physical Non-Linearity (PNL) was considered in relation to the diagrams $M \times N \times 1/r$, and Geometric Non-Linearity (GNL) was calculated following the Newton-Raphson method. Using a typical precast concrete structure with multiple floors and a semi-rigid beam-to-column connection, expressions for a stiffness reduction coefficient are presented. The main conclusions of the study are as follows: the reduction coefficients obtained from the diagram $M \times N \times 1/r$ differ from standards that use a simplified consideration of PNL; the stiffness reduction coefficient for columns in the arrangements analyzed were approximately 0.5 to 0.6; and the variation of values found for stiffness reduction coefficient in concrete beams, which were subjected to the effects of creep with linear coefficients from 0 to 3, ranged from 0.45 to 0.2 for positive bending moments and 0.3 to 0.2 for negative bending moments.

Keywords: precast concrete, physical non-linearity, global stability, $M \times N \times 1/r$ diagrams.

Resumo

No presente trabalho investiga-se a redução da rigidez de elementos estruturais de concreto pré-moldado de edifícios de múltiplos pavimentos para a análise da estabilidade global. Apresentam-se as indicações da redução de rigidez de diferentes códigos, normas e recomendações de associações encontradas na literatura técnica, para servir de comparação com os valores encontrados no estudo. O modelo estrutural analisado foi construído em elementos finitos com o auxílio do software ANSYS®. A não-linearidade física (NLF) foi considerada com as relações dos diagramas $M \times N \times 1/r$ e a não-linearidade geométrica (NLG) segundo o método de Newton-Raphson. Tomando como base uma estrutura típica de concreto pré-moldado de múltiplos pavimentos com ligação viga x pilar de comportamento semi-rígido, são apresentadas expressões para o coeficiente redutor de rigidez. As principais conclusões do estudo desenvolvido são: os coeficientes redutores obtidos segundo o diagrama $M \times N \times 1/r$ divergem das indicações normativas para consideração simplificada da NLF; o coeficiente redutor de rigidez para os pilares dos arranjos analisados foi da ordem de 0,5 a 0,6; a variação dos valores encontrados para os coeficientes redutores de rigidez nas vigas em concreto armado submetidos aos efeitos da fluência pelo coeficiente linear de 0 a 3 foi de 0,45 a 0,2 para momento positivo e de 0,3 a 0,2 para momento negativo.

Palavras-chave: concreto pré-moldado, não-linearidade física, estabilidade global, diagramas $M \times N \times 1/r$.

^a Department of Structural Engineering, São Carlos School of Engineering, University of São Paulo, cuadradomarin@yahoo.com.br, CEP 13566-590, São Carlos, Brazil;

^b Department of Structural Engineering, São Carlos School of Engineering, University of São Paulo, mkdebs@sc.usp.br, CEP 13566-590, São Carlos, Brazil.

1. Introduction

The manufacturing components and industrial conditions involved in producing precast concrete result in numerous advantages, including facilities for quality control, low wastage of materials, and use of high-strength concrete. However, when compared to concrete structures cast on site, the connections between precast components complicates evaluation of structural behavior(s), a situation of particular importance when it comes to global stability analyses of structures with multiple floors.

In general, the Physical Non-Linearity (PNL) and Geometric Non-Linearity (GNL) are taken into account when analyzing the global stability of concrete structures. One of the predominant ways in which PNL is considered in concrete structures is through reducing stiffness in structural elements, as recommended by NBR 6118:2003 [1]. If the beam-to-column connections are perfectly rigid, which is usually the case in concrete structures cast on site, the indications from NBR-6118:2003[1] can be applied. However, the indications from NBR 6118:2003 do not apply when the beam-to-column connections are not perfectly rigid. Few studies in the technical literature regarding precast concrete structures consider conditions of semi-rigid connections. For the case of a pinned beam-to-column connection, Hogeslag [2] recommends a stiffness reduction coefficient (in columns) of 1/3.

Until the last decade of the twentieth century, connections in precast concrete structures were either pinned or rigid. A program in the European Community called COST C1 ("Control of the Semi-Rigid Behavior of Civil Engineering Structural Connections") developed between 1991 and 1998 increased research in this regard for precast concrete structures [3-8]. Since then, the possibility of developing relatively simple beam-to-column connections that have semi-rigid behavior has been investigated in relation to evaluations of global stability for precast concrete structures with multiple floors.

The present study evaluates the reduction of stiffness in structural elements for typical situations involving precast concrete buildings with multiple floors. The study is focused on the case of plane frames with semi-rigid beam-to-column connections and columns embedded in the foundation. The structural arrangements analyzed correspond to the usual modulation(s) and load(s) in multi-storey precast concrete framed structures. The study is performed using the $M \times N \times 1/r$ diagrams for columns and beams, based on NBR 6118:2003 [1]. The GNL is considered in a non-approximated way according to the finite element model, which was constructed using ANSYS® software [9]. The values for the stiffness reduction coefficients obtained are compared with the values recommended by standards and codes found in the technical literature.

2. Values for reduction coefficients in the technical literature

Taking PNL into account, the reduction of stiffness can be defined as follows:

$$EI_{sec} = \alpha E_{ci} I_c \quad (1)$$

where

α represents the stiffness reduction coefficient;

EI_{sec} represents the secant stiffness.

In this section, five recommendations from different codes, standards, and association committees are presented. It should be noted that only some of these recommendations are directed towards precast concrete structures. In principle, the first three pertain to concrete structures cast on site, while the last two pertain to precast concrete.

a) Current Brazilian standard for structural concrete – NBR 6118:2003 [1]

The NBR 6118:2003 [1] allows for an approximate consideration of physical non-linearity to analyze global stability in reticulated structures with at least four floors. For this, the secant stiffness $(EI)_{sec}$, is defined for each element as follows:

$$\text{Slabs: } EI_{sec} = 0.3 E_{ci} I_c \quad (2)$$

$$\text{Beams: } EI_{sec} = 0.4 E_{ci} I_c \quad \text{for } A'_s \neq A_s \quad (3)$$

$$EI_{sec} = 0.5 E_{ci} I_c \quad \text{for } A'_s = A_s \quad (4)$$

$$\text{Columns: } EI_{sec} = 0.8 E_{ci} I_c \quad (5)$$

where

I_c is the moment of inertia of concrete, including, when appropriate, collaborating flange;

E_{ci} is the initial tangent modulus of elasticity;

A_s is the cross-sectional area of tension longitudinal reinforcement;
 A'_s is the cross-sectional area of compression longitudinal reinforcement.

When the bracing frame is composed exclusively of beams and columns and γ_z is less than 1.3, the beams and columns stiffness can be calculated by the following equation:

$$EI_{sec} = 0.7 E_{ci} I \quad (6)$$

The coefficient γ_z is determined from the results of a first-order linear analysis, where it is taken into account the structure's tipping moment and the moment caused by displacement of vertical loads.

b) Committee 318 of the American Concrete Institute - ACI 318-08 [10]

The ACI 318-08 (Building Requirements for Structural Concrete and Commentary) contains two expressions. The first (Eq. 7) is designed for situations with high axial load and small eccentricity values, wherein the effect of slenderness is large. The second (Eq. 8) is a simplified version of the first.

$$EI_{sec} = \frac{0.2E_c I_g + E_s I_s}{1 + \beta_d} \quad (7)$$

$$EI_{sec} = \frac{0.4E_c I_g}{1 + \beta_d} \quad (8)$$

where

E_c is the modulus of elasticity of the concrete. According to ACI, its value is $E_c = 4700\sqrt{f'_c}$, where f'_c is the specified compressive strength of concrete;

E_s is the modulus of elasticity of steel;

I_g is the moment of inertia of concrete in relation to the section's center of gravity without considering reinforcement;

I_s is the moment of inertia of the reinforcement in relation to the section's center of gravity;

β_d is the coefficient related to the creep of concrete and expresses the relationship between the dead axial load and the total axial load. In the case where creep is not considered, $\beta_d = 0$.

c) Bulletin 16 of the Beton International Federation [11]

In Bulletin 16 (Design examples for FIP recommendations 'practical design of structural concrete'), the Beton International Federation (FIB, Federation Internacionale du Beton) presents the following expression for stiffness evaluating:

$$EI_{sec} = \alpha_\varphi \alpha_e E_c I_g + E_s I_s \quad (9)$$

where

$$\alpha_\varphi = 1 - 0.8\varphi(1 - \lambda/200)\omega^{0.25} \quad (10)$$

$$\alpha_e = 0.08\nu_0(0.85f_{cd})^{0.6}e^{(\lambda/100 - 2\omega)} \quad (11)$$

$$\nu_0 = \frac{N_d}{A_c 0.85f_{cd}} \quad (12)$$

$$\omega = \frac{A_{s,tot} f_{yd}}{A_c f_{cd}} \quad (13)$$

and

f_{cd} is the design value of the compressive strength of concrete (MPa);

λ is the slenderness ratio;

φ is the creep coefficient;

$A_{s,tot}$ is the total longitudinal area of steel in the section.

d) Brazilian standard for precast concrete - NBR 9062:1985 [12]

Because the current Brazilian standard for structures of precast concrete (NBR 9062:2006 [13]) does not mention the reduction coefficient for obtaining secant stiffness in columns, it was utilized the previous version of NBR 9062:1985 [12]. The reduction of stiffness in columns on frames with symmetrical reinforcement is, therefore, determined by the following expression:

$$\alpha = 0.2 + 15\rho \quad (14)$$

where

$$\rho = \frac{A_{s,tot}}{bd} \quad (15)$$

e) Committee of the American Institute of precast/prestressed Concrete [14]

The Committee on Prestressed Concrete Columns from the Precast/prestressed Concrete Institute provides the following equation to calculate reduced stiffness in the columns:

$$EI_{sec} = \frac{E_c I_g / \lambda_m}{1 + \beta_d} \quad (16)$$

where:

$$\lambda_m = \theta\eta \geq 3.0 \quad (17)$$

$$\eta = 2.5 + 1.6 \frac{P_0}{P} \Rightarrow 6 \leq \eta \leq 70 \quad (18)$$

$$\theta = \frac{27}{kL/r} - 0.05 \quad (19)$$

and P represents the axial load in the column in a first-order analysis; P_0 represents the maximum acceptable centered load on the column; K represents the coefficient of effective length of the column considering the boundary conditions; L represents the length of the column; r represents the radius of gyration of the cross section.

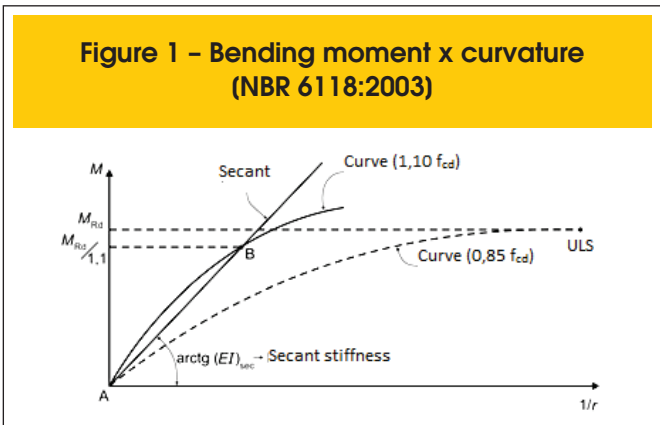
In this case, it is noteworthy that the expression takes into account the geometric characteristics and connections in the structural elements.

As shown by Table 1, a comparative table of the factors considered in each recommendation, a) there is a large difference between the factors considered and b) NBR 6118:2003 [1] is the only scenario with fixed values. It is important to note that the factors considered are only applied to columns.

3. Models for analysis

The precast concrete structure considered in this study was modeled as a plane frame, using ANSYS® software [9] for structural analyses with finite elements. The non-simplified consideration of PNL implies knowing the $M \times N \times 1/r$ diagram (in other words, the stiffness) for each section in which there is a change in stress, cross-section, reinforcement, concrete cover, and strength of concrete. Thus, structures that are discretized into a greater number of finite elements have more representative solutions. Using the ANSYS® software [9], the constitutive relationship between beams and columns can be represented by the $M \times N \times 1/r$ diagram using the beam element BEAM188.

The discretization adopted for modeling the structure through the finite element method employed 8 finite elements for each column section, where each section corresponds to the region between floors. With regard to the beams, 16 finite elements were used for each beam section, where each section was defined by the region between corbels. The corbels were discretized into a finite element, and the stiffness of the corbels was defined by the product $E_c I_c$. The elements of connection were modeled using COMBIN39, permitting the bending moment x rotation relationship to be represented in a non-linear and asymmetric way.



The GNL was analyzed according to the complete Newton-Raphson method. Displacement control was the criterion used to determine when the iterative process was stopped. The defined tolerance was 0.5%, meaning that the iterative process was interrupted when there the increase in displacement relative to the previous iteration was no more than 0.5%. The non-linear analysis was performed by dividing the load into 10 steps.

According to NBR 6118:2003 [1], non-linearity can generally be considered through each section's bending moment x axial force x curvature relationships ($M \times N \times 1/r$ diagrams), where the reinforcement and acting axial force are supposedly known. NBR 6118:2003 [1] describes two ways of using the $M \times 1/r$ diagram; the first is designed for the ultimate limit state, and the second is designed for evaluating the secant stiffness of the elements. Figure 1 shows the $M \times 1/r$ diagram from NBR 6118:2003 [1].

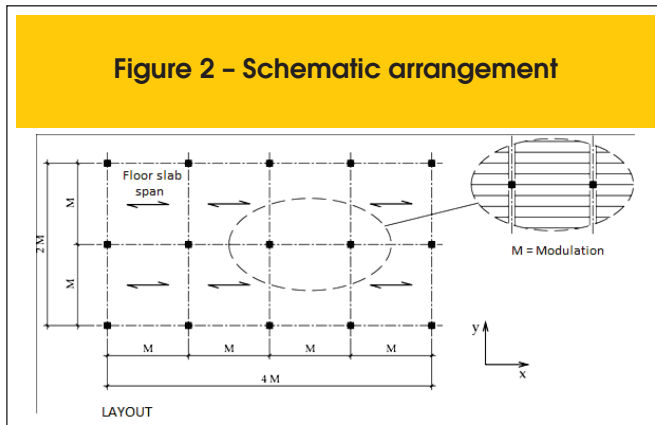
According to NBR 6118:2003 [1], to calculate ULS, the design value of the compressive strength of concrete should be multiplied by 0.85. As explained by CARVALHO and FIGUEIREDO [15], because the concrete shows greater compressive strength in short-term trials, the value of $0.85 f_{cd}$ is assigned to the duration of the compressive strength tests. In typical structures, the load continues to act on the structure throughout its entire useful life. Under dead load, concrete's compressive strength decreases over time, a phenomenon called the Rüsçh effect.

According to FRANÇA [16], calculating the stiffness from constitutive relationships based on design values of the concrete strength can lead to overestimating the effects of non-linearity. To account for stiffness, the design value of the concrete compressive strength should be multiplied by 1.10. This coefficient considers the fact

Table 1 - Factors considered in each recommendation

	VALUES	AXIAL FORCE	CREEP	REINFORCEMENT	SLENDERNES
NBR 6118:2003	FIXED	NO	NO	NO	NO
ACI 318-08	VARIABLE	NO	YES	YES	NO
FIB (2002)	VARIABLE	YES	YES	YES	YES
NBR 9062:1985	VARIABLE	NO	NO	YES	NO
PCI (1988)	VARIABLE	YES	YES	NO	YES

Figure 2 – Schematic arrangement



that not all of the sections in the structural element are made from materials with values corresponding to lower statistical quantiles. In other words, not all of the sections in the element are equally affected by the conditions taken into account by coefficient γ_m , which considers the weights of strengths.

Regarding the safety of the loads, the second-order analyses were performed using the $M \times N \times 1/r$ diagram(s). NBR 6118:2003 [1] suggests using a formula for safety in which the loads are increased by γ_f/γ_{f3} . After determining the second-order effects, the loads are increased by γ_{f3} , with $\gamma_{f3}=1.1$. According to NBR 8681:2003 [17], the coefficient γ_{f3} considers the possible errors in evaluating the effects of the loads, whether from constructive problems or from deficiencies in the calculation method used.

Secant stiffness is calculated as follows: a) first, the resistant moment in the transversal section (M_{rd}) is calculated, using a value of $0.85f_{cd}$ for stress on the concrete, and the acting load is increased by $\gamma_f(N_d)$; b) next, the $M \times N \times 1/r$ diagram is constructed using a value of $1.1f_{cd}$ for stress on the concrete, and the acting load is increased by $\gamma_f/\gamma_{f3}(N_d/\gamma_{f3})$. The secant stiffness is defined by the relationship between the resistant moment (M_{rd})/ γ_{f3} and the corresponding curvature in the $M \times N \times 1/r$ diagram constructed with a value of $1.1f_{cd}$ of stress on the concrete and acting load increased by $\gamma_f/\gamma_{f3}(N_d/\gamma_{f3})$.

The combined effects of the intact concrete between cracks and the concrete's tensile strength constitute a phenomenon known as "tension stiffening". The manual from fib [18] accounts for this effect with regard to the relationship $M \times 1/r$. However, this effect is not taken into account in the present study.

The procedures used here are valid for experimental verifications of concrete with f_{ck} values up to 50 MPa, the maximum strength grade for which NBR 6118:2003 [1] is applicable. Construction of the $M \times N \times 1/r$ diagram is accomplished by determining the axial strength force (v_{rd}) that is able to balance a pre-fixed axial force (v_{fixo}). Because the pre-fixed axial force is associated with a curvature and neutral position, this procedure is necessarily incremental and iterative. After defining the neutral axis, the dimensionless resistant moment is calculated. The procedure used to construct the $M \times N \times 1/r$ diagram and a description of the incremental and iterative process can be found in the study by MARIN [19]. The $M \times N \times 1/r$ diagrams can be shown as dimensionless values. The study of FUSCO [20] details the relationships between the dimensionless bending moment (μ), the dimensionless axial force (v), and curvature (d/r) that can be found for different d/h relationships and

grades of steel. The study of OLIVEIRA [21] contains abacuses that relate the dimensionless bending moment, the dimensionless axial force, and the secant stiffness adjusted for the effect of the linear creep coefficient.

The results obtained in MARIN [19] for the resistant moment and secant stiffness were compared with the values found in the abacuses developed by OLIVEIRA [20], with differences of approximately 1%. The values shown in the abaci by FUSCO [20] were also compared with those obtained by MARIN [19], with differences of approximately 1%.

4. Numerical simulations in the representative cases

The analysis herein was performed using a structural arrangement representative of multi-storey precast concrete buildings. Figure 2 shows the schematic arrangement with modulations of 7.5 m and 10 m.

The structural system used in the present study is constituted by frames with semi-rigid beam-to-column connections and columns embedded in the foundation. As illustrated in Figure 3, this beam-to-column connection is formed by two bolts and concrete topping cast on site, with reinforcement passing through the central columns. On the end columns, the reinforcement for negative bending moments is anchored in mechanical splices. For any direction in which there is no column-beam plane, the stability must be ensured by the stiffness in the columns. Horizontal wind loads are transferred to the other components by the slab, which behaves like a diaphragm. Thus, a central frame in direction y was selected, as shown in Figure 2, as an object of study.

The semi-rigid behavior of the beam-to-column connection was taken into account using the bending moment \times rotation of connection proposed in El Debs et al. [22], which is reproduced in Figure 4.

Using the semi-rigid beam-to-column connection, the increasing of floors number typically used with pinned connections (3 floors, approximately 12 m in height) was investigated. Based on preliminary calculations, which were subsequently proven, the beam-to-column connection allowed for increasing the number of floors to 6 when the column's cross section was 50 cm \times 50 cm for a modulation of 7.5 m and 60 cm \times 60 cm for a modulation of 10 m. For both

Figure 3 – Beam-to-column connection

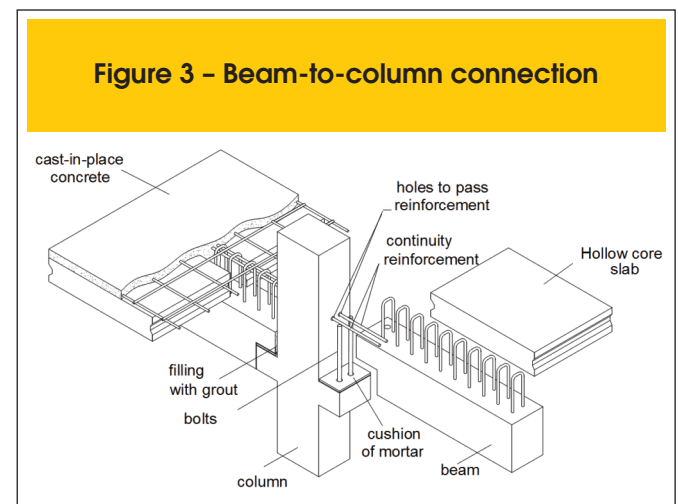
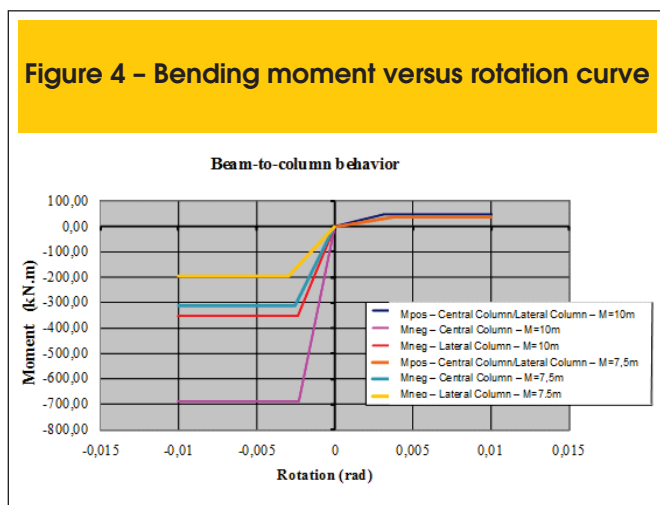


Figure 4 – Bending moment versus rotation curve



modulations, buildings with up to 4 floors were stable for column cross-sections of 40 cm x 40 cm.

Based on the above considerations, the variables and parameters described below were analyzed.

a) Number of floors (height): 4 floors (16 m), 5 floors (20 m), and 6 floors (24 m).

b) Materials: concrete C-35 ($f_{ck}=35$ MPa), steel CA-50 for longitudinal reinforcement, and steel CA -60 for cross-sectional reinforcement.

c) Cross-sectional and longitudinal reinforcement in the columns (according to Table 2): the longitudinal reinforcement ($A_{s,tot}$) was uniformly distributed in the sides of the section, and the geometric rate of reinforcement corresponded to approximately 3% of all the sections of the columns. The cross-sectional reinforcement consisted of stirrups with a diameter of 6 mm; and a minimum concrete cover of 2.5 cm for the cross-sectional reinforcement in the columns was adopted.

d) Dead loads: the self-weight of the hollow core slab was 2.2 kN/m² for a span of 7.5 m and 2.6 kN/m² for a span of 10 m. The structural concrete topping 6 cm thick, with a self-weight of 1.5 kN/m² and a coating of 0.5 kN/m². The average thickness of the structural concrete topping was 6 cm (considering the upward deflection of the hollow core slabs); and, for all cases, a load of 10 kN/m per floor (resulting from the masonry's self-weight) was used around the perimeter of the structure.

e) Live loads: two values, - 3 and 5 kN/m², were considered.

f) Wind pressure: wind pressure was calculated according to NBR 6123:1988 [23]. The force of wind on a given structural arrangement was broken down according to the number of floors and height, as shown in Table 3, for the case study corresponding to the central frame with a modulation of 7.5 m.

g) Load combinations: three load combinations were considered for ULS: in the first, which employed a high concentration of people in a typical commercial, public, or office building, the wind's load was the main load, and the live load was considered secondary (this combination was important to verify the global stability of the structure as a whole). The second combination did not consider the contribution of the live load (its verification was extremely important due to the positive moment caused by the wind on connections). In the third load combination, the live load was predominant, and the load from the wind was secondary.

Thus, three expressions for load combinations for the ultimate limit state are obtained, as shown below:

$$F_{d,1} = \gamma_g \cdot G + 1.4(W + 0.7Q) \quad (20)$$

$$F_{d,2} = \gamma_g \cdot G + 1.4W \quad (21)$$

$$F_{d,3} = \gamma_g \cdot G + 1.4(0.6W + Q) \quad (22)$$

where:

G represents dead loads;

Q represents live loads;

W represents wind loads.

The wind load was considered in all combinations; therefore, the no-bearing walls were finished. The axial force on the columns on each floor were calculated based on the values of the loads considered. Table 4 presents the values for all cases for a modulation of 7.5 m and live load of 3 kN/m².

The axial force is shown in dimensionless form in Table 5. This form of presentation facilitates the association between the increase in axial force and the increase in the element's stiffness.

The loads acting on the structure were defined according to each load combination. Once the loads acting on the structure were defined, the beam and column were characterized with the help of the $M \times N \times 1/r$ diagrams, which were built using calculation tools developed in MARIN [19]. In this way, the strength and stiffness of the elements were determined.

Table 2 – Cross sections in the structural arrangements

Cross section (cm x cm)	$A_{s,tot}$ (cm ²)	M (m)	N° floors
40x40	50.4 (16 Φ 20 mm)	7.5 e 10	4
50x50	75.6 (24 Φ 20 mm)	7.5	5 e 6
60x60	120.0 (24 Φ 25 mm)	10	5 e 6

Table 3 – Characteristic wind loading for modulation with 7.5m

Wind Load - Direction Y												
h(m)	Modulation 7.5m			6 FLOORS			5 FLOORS			4 FLOORS		
	S ₂	V _k (m/s)	q (kN/m ²)	H/L1	C _a	F _o (kN)	H/L1	C _a	F _o (kN)	H/L1	C _a	F _o (kN)
4	0.76	34.20	0.717	0.80	1.24	28.11	0.67	1.21	27.43	0.53	1.18	26.75
8	0.80	36.00	0.794	0.80	1.24	31.46	0.67	1.21	30.70	0.53	1.18	29.94
12	0.85	38.25	0.897	0.80	1.24	34.97	0.67	1.21	34.12	0.53	1.18	33.28
16	0.89	40.05	0.983	0.80	1.24	37.41	0.67	1.21	36.50	0.53	1.18	37.40
20	0.91	40.95	1.028	0.80	1.24	39.09	0.67	1.21	39.09	0.53	1.18	39.09
24	0.93	41.85	1.074	0.80	1.24	39.97	0.67	1.21	39.97	0.53	1.18	39.97

h.: Floor height; H: Structure height ; V_k: Characteristic wind speed; S₂: Factor used in V_k; q: Wind pressure; L1: Structure length; C_a: Pressure coefficient; F_o: Wind Load.

Table 4 – Axial force in columns (P50x50) for structure with modulation 7.5m and live load 3 kN/m²

FLOOR	N _{d,1} (kN)		N _{d,2} (kN)		N _{d,3} (kN)	
	CC	LC	CC	LC	CC	LC
6	534.94	318.65	330.19	216.28	605.81	354.00
5	1069.88	742.31	660.38	537.56	1211.62	813.09
4	1604.82	1165.96	990.57	858.84	1817.44	1272.19
3	2139.75	1589.62	1320.75	1180.12	2423.25	1731.28
2	2674.69	2013.28	1650.94	1501.41	3029.06	2190.38
1	3209.63	2436.93	1981.13	1822.69	3634.87	2649.47

CC (Central Column); LC (Lateral Column);
 N_{d,1}: Axial force for 1st load combination in ULS, where the wind load was taken as main;
 N_{d,2}: Axial force for 2nd load combination in ULS, where the wind load was taken as single load;
 N_{d,3}: Axial force for 3rd load combination in ULS, where the live load was taken as main.

The model created in ANSYS® [9] was motivated by the evaluation of global stability in the structural arrangements studied. The structural arrangements show different shapes, cross-sections of the elements, and loads. In addition, the semi-rigid behavior of the beam-to-column connection was considered. The model accounted for PNL while using finite element BEAM188, enabling the relationship M x N x 1/r to be calculated. To evaluate the stabilities of the arrangements, the γ_z coefficients were calculated from the displacements obtained in the process. These values varied from 1.05 to 1.20, indicating that the degree of PNL in the models analyzed was not significant.

In models with non-linearity, there were variations in the configurations of the axial forces on the columns because of the non-linear processes. In the model analyzed there are GNL, PNL, and non-linearity in the beam-to-column connection that has asymmetric behavior.

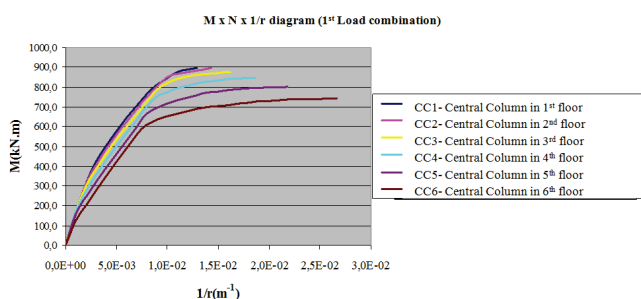
Changes in the axial forces on the columns would necessitate an iterative analysis in the construction of the M x N x 1/r diagram.

Table 5 – Dimensionless axial force in columns (P50x50) for structure with modulation 7.5m and live load 3 kN/m²

FLOOR	V _{d,1}		V _{d,2}		V _{d,3}	
	CC	LC	CC	LC	CC	LC
6	0.09	0.05	0.05	0.03	0.10	0.06
5	0.17	0.12	0.11	0.09	0.19	0.13
4	0.26	0.19	0.16	0.14	0.29	0.20
3	0.34	0.25	0.21	0.19	0.39	0.28
2	0.43	0.32	0.26	0.24	0.48	0.35
1	0.51	0.39	0.32	0.29	0.58	0.42

$$V_{d,i} = \frac{N_{d,i}}{A_c \cdot f_{cd}} \text{ : Dimensionless axial force}$$

Figure 5 – M x N x 1/r diagram for first load combination in central column P50x50



Because the present study did not consider the effect of such axial force variations, the M x N x 1/r diagrams were constructed and used in the finite element model in one step. Initially, the stiffness of elements in a precast concrete building with 6 floors was analyzed. According to the above methodology, the reference bending moment for evaluating the stiffness reduction in the elements depends on the resistant moment in the section and not on the loads acting on the element.

For each section of the elements in the study, M x N x 1/r diagrams were constructed and analyzed, and the stiffness reduction coefficients were found. Functions to reduction stiffness related to the stiffness reduction coefficient and the dimensionless axial force are proposed. The reduction coefficients found using the stiffness functions recommended by different standards are compared with the values found from the M x N x 1/r diagrams.

After defining the value of the axial force and the load combinations acting on a section of a column, the M x N x 1/r diagrams were calculated. Figure 5 shows an example of a diagram using a stress value (on the concrete) of $1.1 f_{cd}$ and increasing the acting loads by $\gamma_f (N_d)$. Table 6 shows the coefficients obtained from the M x N x 1/r diagram that used a stress value (on the concrete) of $1.1 f_{cd}$ and increased the acting loads by $\gamma_f / \gamma_{f3} (N_d / \gamma_{f3})$. This enabled the determination of the stiffness reduction coefficients corresponding to secant stiffness.

Analyzing the stiffness reduction coefficients shown in Table 6 with respect to the calculation combinations in ULS, the central column's stiffness reduction coefficient varied from approximately 0.35 to 0.6, and the lateral column's coefficient varied from approximately 0.35 to 0.5. Because of the greater effect of the axial force in the third combination, the stiffness reduction coefficient found in the third combination of loads is greater than the stiffness reduction coefficients found in the first and second combination.

Table 6 – Stiffness reduction coefficient in columns (P50x50) for structure with modulation 7.5m and live load 3 kN/m²

FLOOR	$\alpha_{,1}$		$\alpha_{,2}$		$\alpha_{,3}$	
	CC	LC	CC	LC	CC	LC
6	0.366	0.343	0.345	0.333	0.375	0.347
5	0.430	0.397	0.384	0.366	0.446	0.404
4	0.493	0.441	0.422	0.409	0.501	0.453
3	0.514	0.492	0.459	0.443	0.527	0.498
2	0.539	0.509	0.495	0.483	0.566	0.516
1	0.583	0.528	0.507	0.501	0.625	0.538

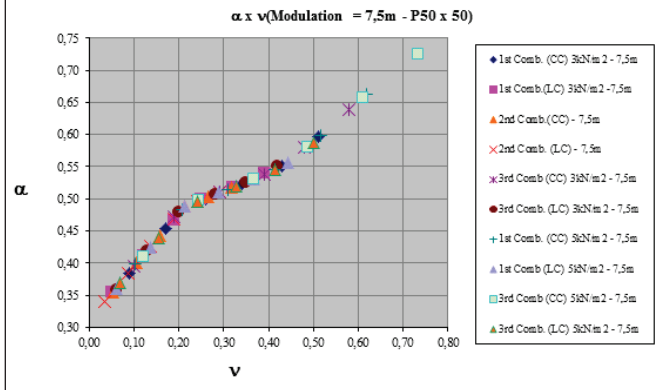
$\alpha_{,1}$: Stiffness reduction coefficient in columns for 1st load combination (ULS);
 $\alpha_{,2}$: Stiffness reduction coefficient in columns for 2nd load combination (ULS);
 $\alpha_{,3}$: Stiffness reduction coefficient in columns for 3rd load combination (ULS).

Table 7 – Stiffness reduction coefficient calculated in each recommendation

ν	λ	M x N x 1/r	NBR 6118:2003	ACI 318-08	FIB	NBR 9062:1985	PCI
0.58	27.71	0.625	0.800	0.471	0.429	0.758	0.162
0.58	63.74	0.625	0.800	0.471	0.498	0.758	0.038
0.03	27.71	0.333	0.500	0.471	0.280	0.758	0.015
0.03	63.74	0.333	0.500	0.471	0.283	0.758	0.038

ν : Dimensionless axial force; λ : Slenderness ratio.

Figure 6 – Diagram of stiffness reduction coefficient versus dimensionless axial force for columns (P50x50) in structures with modulation of 7,5 m with live load 3 kN/m² and 5 kN/m²



Next, the values found for stiffness reducing according to the $M \times N \times 1/r$ diagram were compared with the values obtained from the approximate functions recommended by standards. Two limiting situations based on the axial force and the slenderness are considered. With regard to the axial force, the maximum and minimum axial force of the load combinations were considered. With regard to the slenderness, two hypotheses are considered because the beam-to-column connections studied behave as semi-rigid. In the first, the effective length of the column corresponded to the difference in height between floors. In the second, the effective length corresponded to the maximum value indicated for precast concrete structures with multiple floors that are unbraced. According to Elliott [24], this value is at least 2.3 times that of the height difference between floors. Table 7 presents the reduction coefficients obtained from the recommendations in the technical literature. The effects of creep on the columns were not considered. Thus, the creep coefficient $\varphi=0$

Figure 7 – Functions for reducing stiffness versus dimensionless axial force for columns (P50x50)

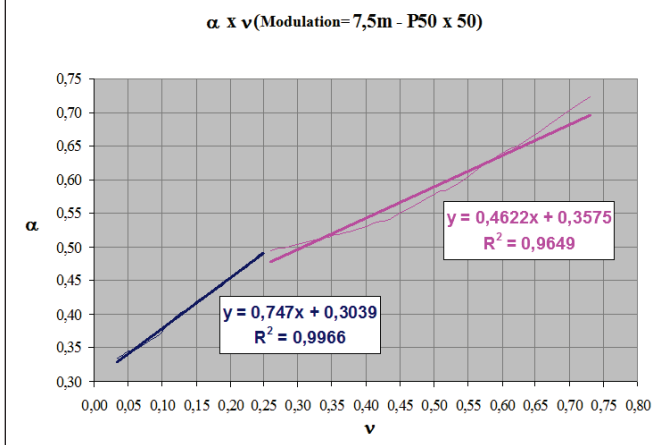


Table 8 – Functions for reducing stiffness according to subdomains in dimensionless axial force for columns (P50x50)

Stiffness reduction function	Subdomain (v)
$\alpha = 0.75 v + 1.10 (E_S I_S) / EI$	$0 \leq v \leq 0.25$
$\alpha = 0.46 v + 1.32 (E_S I_S) / EI$	$0.25 < v \leq 0.75$

in the construction of the $M \times N \times 1/r$ diagram and in the expression from FIB [11] are used. Based on the formulas recommended by ACI 318-08 [10] and PCI [14], β_d was 0.

The reduction coefficient recommended by NBR 6118:2003 [1] for columns is 0.8, while that for beams with symmetric reinforcement is 0.5. The reduction-coefficient variations depicted in Table 6 indicate no correspondence between the values found herein and the reduction coefficients suggested for columns in NBR 6118:2003 [1]. Considering that due to the low-level axial force, the behavior of columns on the 6th floor is very similar to that of beams, the coefficient recommended by NBR 6118:2003 [1] can be interpreted as 0.5. However, with symmetrical reinforcement, the value of the reduction coefficient determined from the $M \times N \times 1/r$ diagram is approximately 0.35.

The reduction coefficient obtained according to NBR 9062:1985 [12] does not agree with the values obtained for the stiffness reduction coefficient from the $M \times N \times 1/r$ diagram, indicating that the latter is inadequate for the example studied. The values obtained according to ACI 318-08 [10] correspond well to the intermediate sections of the column and, when compared to recommendations from standards, the modulus of elasticity was the same as NBR 6118:2003 [1].

The procedure presented by PCI [14] and FIB [11] consider the slenderness of the column. However, considering the slenderness of the

Figure 8 – Diagram of stiffness reduction coefficient versus dimensionless axial force for columns (P40x40) in structures with modulation (7.5 m; 10 m) and live load (3 kN/m²; 5 kN/m²)

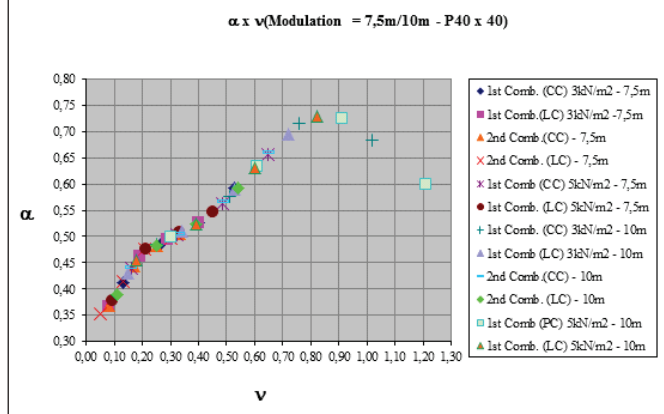
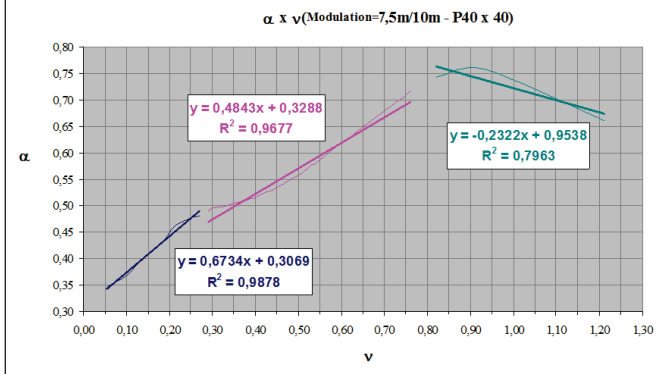


Figure 9 – Functions for reducing stiffness versus dimensionless axial force for columns (P40x40)



column makes the analysis more complex because of the semi-rigid connection and, consequently, the displacement of the structure. The values obtained for the stiffness reduction coefficient according to PCI [14] for the two slenderness situations did not agree with the values obtained from the $M \times N \times 1/r$ diagram. The values found from FIB [11] for dimensionless axial force equal to 0.03, were close to the values found with the $M \times N \times 1/r$ diagram.

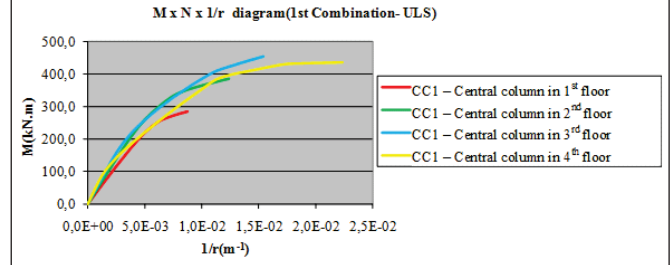
The rate and arrangement of the reinforcement as well as the value of the axial force have a higher degree of influence in the present analysis. The analysis of secant stiffness occurs in each section of the element, and the slenderness of the element is related to the analysis of the element's stiffness as a whole.

The study for obtaining stiffness was performed for a structure with 6 floors and live load of 3 kN/m² was also done for a live load with 5 kN/m², as observed in the diagram of stiffness reduction coefficients shown in Figure 6. Each data series shown in Figure 6 has 6 points. Each point corresponds to a stiffness reduction coefficient associated with a floor.

Figure 7 shows two approximations with linear variation divided into two sub-domains. Functions for reducing stiffness according to the respective sub-domains are proposed, as presented in Table 8. It should be noted with a value of approximately 0.25 for dimensionless axial force, there is a change in the rate of the element's increase in stiffness.

The same procedure was performed for columns with cross-sections

Figure 10 – M x N x 1/r diagram for first load combination in central column P40x40



tions of 40 x 40 cm and 60 x 60 cm. This report depicts only the study designed for the columns with a 40 x 40 cm cross-section because, in this case, the variation of stiffness decreases upon reaching a certain level of axial force. Figure 8 shows the variation in the stiffness reduction coefficient according to the dimensionless axial force and the modulations and loads to which the columns (40 x 40 cm) were subjected.

In Figure 9, it is possible to evaluate the variation in stiffness reduction coefficients according to the three sub-domains and, respectively, the three approximate functions. The portion associated with reinforcement in the reduction stiffness coefficient has a value of 0.26 when the reinforcement's area and provision is P(40x40). According to the $M \times N \times 1/r$ diagram, the reduction coefficient associated with zero dimensionless axial force is equal to 0.319.

For the column with a cross-section of 40 x 40 cm, the stiffness decreased when the value of the dimensionless axial force reached 0.9. This behavior was not observed for other column sections because the axial force level was lower. Figure 10 shows the $M \times N \times 1/r$ diagram (for the column with a 40 x 40 cm section), which was constructed with a concrete stress of 1.1 f_{cd} and increasing acting loads by γ_f / γ_{f3} (N_d / γ_{f3}), a modulation of 10 m, and a live load of 5 kN/m².

Table 9 presents proposed functions for reducing stiffness according to respective sub-domains for columns with sections of 40 x 40 cm, 50 x 50 cm, and 60 x 60 cm. Additionally, a function for reducing average stiffness for each section studied are proposed. The numerical simulations were designed based on different column cross-sections, according to the number of floors and the

Table 9 – Functions for reducing stiffness according to sub-domains in dimensionless axial force for columns (P40x40, P50x50, P60x60)

Cross Section (cm)	Stiffness reduction function (α)		
	$0 \leq v \leq 0.25$	$0.25 < v \leq 0.85$	$0.85 < v \leq 1.20$
40 x 40	$0.67v + 1.15(E_s I_s)/EI$	$0.48v + 1.20(E_s I_s)/EI$	$-0.24v + 3.50(E_s I_s)/EI$
50 x 50	$0.75v + 1.10(E_s I_s)/EI$	$0.46v + 1.32(E_s I_s)/EI$	-----
60 x 60	$0.73v + 1.12(E_s I_s)/EI$	$0.44v + 1.29(E_s I_s)/EI$	-----
Average value	$0.72v + 1.12(E_s I_s)/EI$	$0.46v + 1.27(E_s I_s)/EI$	$-0.24v + 3.50(E_s I_s)/EI$

Table 10 – Distribution of stiffness reduction coefficient in columns

Modulation	Cross Section	N° Floors	Live load (kN/m ²)	α
7.5	50 x 50	6	3	0.35 - 0.60
7.5	50 x 50	6	5	0.35 - 0.70
10.0	60 x 60	6	3	0.40 - 0.70
10.0	60 x 60	6	5	0.40 - 0.77
7.5	40 x 40	4	3;5	0.35 - 0.65
10.0	40 x 40	4	3;5	0.40 - 0.76

modulation used. Table 10 shows the intervals of stiffness reduction coefficients obtained for the columns in the models analyzed. The lowest values correspond to the highest floors, and the highest values correspond to the lowest floors. For the average values, the reduction coefficients range from 0.5 to 0.6. These coefficients are smaller than the values recommended by NBR 6118:2003 [1], which are 0.7 to 0.8.

The effects of adopting prestressing steel and non-prestressing steel in the precast concrete beams arranged on the central axis of the lay-out showed in the Figure 2 are also evaluated. Figure 11 shows the section of the precast concrete beam used in all the floors with $f_{ck}=35$ MPa and a section composed of topping with $f_{ck}=20$ MPa. The non-prestressing steel uses steel CA-50. Only the main reinforcement was used in constructing the M x N x 1/r diagram. Figure 12 shows the M x N x 1/r diagram for the beam, which is shown in Figure 11, with a linear coefficient of creep equal to 0 and 2. In constructing the M x N x 1/r diagram, due to the

Figure 12 – M x N x 1/r diagram in composite reinforced beam for structure with modulation 7.5m

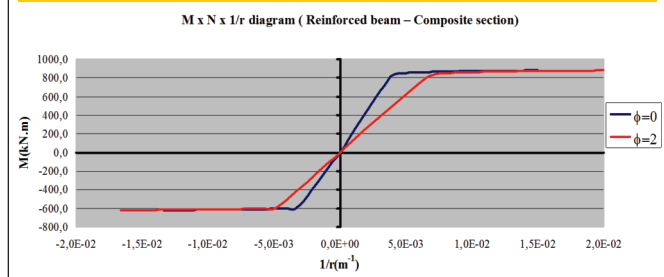


Figure 11 – Cross sectional and reinforcement arrangement of composite reinforced beam for structure with modulation 7.5m

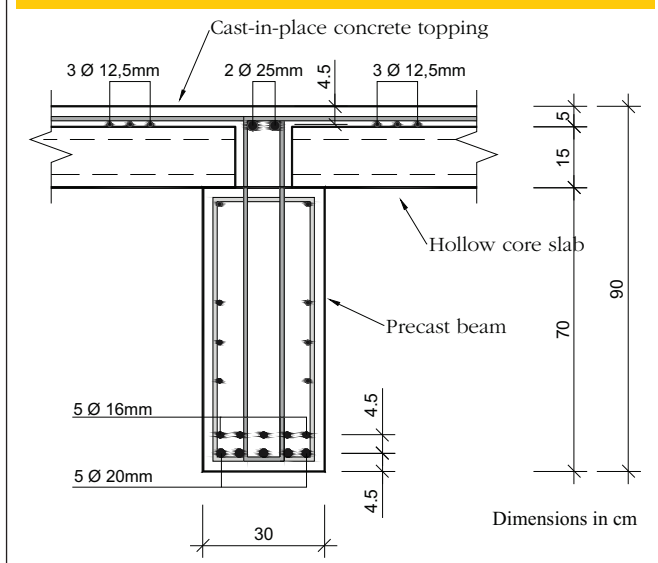


Table 11 – Stiffness reduction coefficient in composite reinforced beam for structure with modulation 7.5m and creep effect

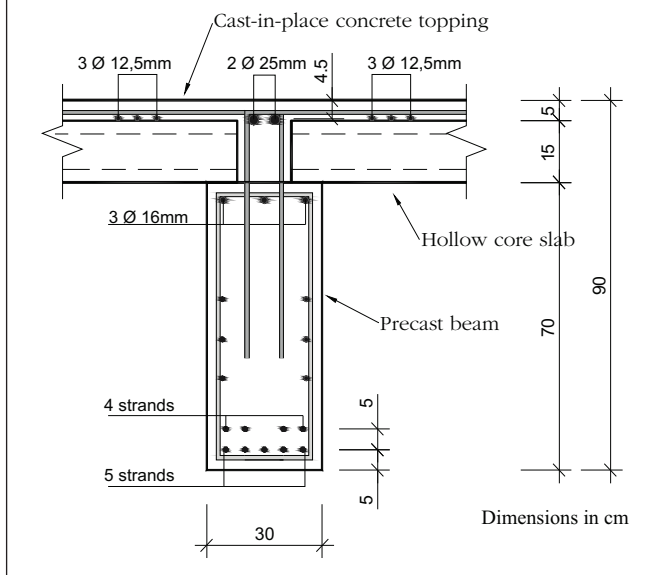
Creep coefficient (ϕ)	0	1	2	3
$M_{pos} (\alpha)$	0.467	0.340	0.267	0.220
$M_{neg} (\alpha)$	0.310	0.249	0.209	0.180

strength differences between beams made of precast concrete and those made with concrete cast on site, the section related to positive bending moment was built with $f_{ck}=20$ MPa, and the section related to negative bending moment was built with $f_{ck}=35$ MPa. Table 11 shows the stiffness reduction coefficient versus the coefficient of creep for positive bending moment and negative bending moment. The significant decrease in the stiffness reduction coefficient as it relates to the progression of creep can be notice.

The reduction coefficient shown by NBR 6118:2003 [1] for beams with asymmetrical reinforcement is 0.4, a value similar to that found for scant stiffness with positive bending moment and a linear coefficient of creep equal to 0.

Figure 13 summarizes the evaluation of the effect of using prestressing steel in the cross-section of the precast concrete beam.

Figure 13 – Cross sectional and reinforcement arrangement of composite prestressed beam for structure with modulation 7.5m



The precast concrete beam has $f_{ck} = 40$ MPa, and the concrete cast on the site has $f_{ck} = 20$ MPa. Prestressing steel of the section is made of strands CP 190 RB 12.7, and non-prestressing steel is made of steel CA-50.

Figure 14 shows the $M \times N \times 1/r$ diagram, which is modified for prestressing steel, and Table 12 shows the stiffness reduction coefficients obtained using prestressing steel on the section bottom and non-prestressing steel on the upper part of the beam.

5. Final remarks and conclusions

Based on the cross-sections, arrangements, reinforcement rates, and materials used in this study, the following conclusions can be drawn:

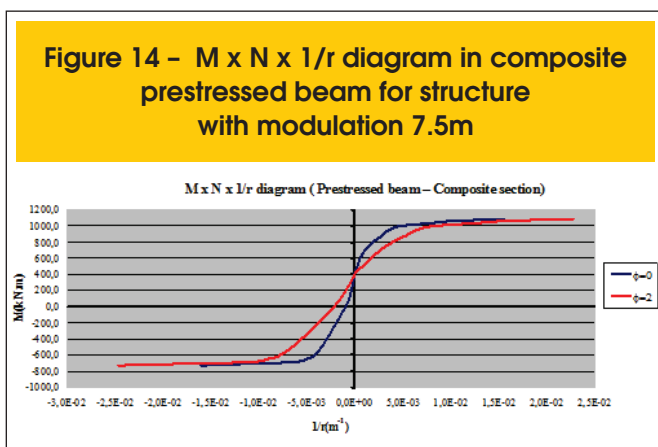


Table 12 – Stiffness reduction coefficient in composite prestressed beam for structure with modulation 7.5m and creep effect

Creep coefficient (ϕ)	0	1	2	3
$M_{pos}(\alpha)$	0.570	0.402	0.311	0.253
$M_{neg}(\alpha)$	0.211	0.150	0.116	0.095

- The procedures and recommendations of national codes regarding the simplified consideration of PNL are less comprehensive than the procedures and recommendations of international codes.
- The reduction coefficients obtained from the $M \times N \times 1/r$ diagram differ from the normative indicators obtained with a simplified PNL, mainly due to the effects of creep, axial force, and prestressing steel. The reduction coefficients are influenced by the levels of axial force and, consequently, vary according to the combination of loads used.
- The rate of increase in stiffness changes when the value of the axial force is approximately 0.25.
- According to the studies performed, increasing the level of the axial force increases the stiffness of the sections. However, the section's stiffness decreases after reaching a threshold value of axial force. In the numerical simulation evaluated herein, a value for the dimensionless axial force of approximately 0.9 is obtained and a reversal in the trend of increasing stiffness is observed.

The following conclusions are limited to the structural arrangements, loads, and type of connection used in the structural system studied herein. They serve as a basis of comparison with the coefficients of stiffness from NBR 6118:2003 [1] as follows:

- The stiffness reduction coefficients obtained for columns with the arrangements analyzed herein showed average values from 0.5 to 0.6.
- The values found for the stiffness reduction coefficients in the concrete beams, which were subjected to the effects of creep with a linear coefficient of 0 to 3, varied from 0.45 to 0.2 for positive bending moment and 0.3 to 0.2 for negative bending moment. In the elements with prestressing steel, the reduction coefficients obtained ranged from 0.55 to 0.25 for positive bending moment, and from 0.25 to 0.1 for negative bending moment.

It is important to notice that the purpose of this study was to investigate stiffness reduction for a typical case study that has a multi-storey precast concrete structure and a particular semi-rigid connection. Therefore, the conclusions are limited, however, they can be useful for comparisons with values from NBR 6118:2003 [1].

6. Acknowledgements

We are grateful to LEONARDI Industrialized Construction for its developmental support of this research and to the Foundation for Research Support in the State of São Paulo (FAPESP – Fundação de Amparo a Pesquisa do Estado de São Paulo) for its help with the thematic research project that encompassed this study.

7. References

- [01] ASSOCIAÇÃO BRASILEIRA DE NORMAS TÉCNICAS. NBR 6118 (2003). NBR 6118: Projeto de estruturas de concreto - Procedimento. Rio de Janeiro.
- [02] HOGESLAG, A. J. (1990). Stability of precast concrete structures. In: HOGESLAG, A. J.; VAMBERSKY, J. N. J. A.; WALRAVEN, J. C. Prefabrication of concrete structures (Proc. Int. Seminar Delft, The Netherlands, October, 25-26, 1990). Delft: Delft University Press, 1990. p.29-40.
- [03] CHEFDEBIEN A. de & DALDARE J. (1994). Experimental investigations on current connections between precast concrete components. COST C1 Proc. of 2nd Workshop Semi-rigid Behaviour of Civil Engineering Structural Connections, Prague, p. 21-30.
- [04] ELLIOTT, K. S.; DAVIES, G.; MAHDI, A.; GORGUN, H.; VIRDI, K. & RAGUPATHY P. (1998). Precast concrete semi-rigid beam-to-column connections in skeletal frames. COST C1 Proc. of The International Conference, Control of Semi-rigid Behaviour of Civil Engineering Structural Connections, Liège, p. 45-54.
- [05] KERONEN A. & HIETALA J. (1998). Tests and analysis of the connections in precast concrete portal frame. COST C1 Proc. of The International Conference, Control of Semi-rigid Behaviour of Civil Engineering Structural Connections, Liège, p. 25-34.
- [06] CHEFDEBIEN, A. de (1998). Precast concrete beam to column head connections. COST C1 Proc. of The International Conference, Control of Semi-rigid Behaviour of Civil Engineering Structural Connections, Liège, p. 35-43.
- [07] ELLIOTT, K.S.; DAVIES, G.; FERREIRA, M.. GORGUM, H.; MAHADI, A.A. (2003a). Can precast concrete structures be designed as semi-rigid frames? Part 1: The experimental evidence. The structural engineer. v.81, n.16 p. 14-27.
- [08] ELLIOTT, K.S.; DAVIES, G.; FERREIRA, M.. GORGUM, H.; MAHADI, A.A. (2003b). Can precast concrete structures be designed as semi-rigid frames? Part 2: Analytical equations & column effective length factors. The structural engineer. v.81, n.16 p. 28-37
- [09] ANSYS RELEASE 10.0 (2005). Documentation for Ansys. 1st ed. Chicago, USA.
- [10] AMERICAN CONCRETE INSTITUTE (2008). ACI 318-08: Building Code Requirements for Structural Concrete and Commentary. Farmington Hills.
- [11] FÉDÉRATION INTERNACIONALE DU BETON (2002). Design examples for FIP recommendations ' practical design of structural concrete', Bulletin FIB, Lausanne, v.16.
- [12] ASSOCIAÇÃO BRASILEIRA DE NORMAS TÉCNICAS. NBR 9062 (1985). NBR 9062: Projeto e execução de estruturas de concreto pré-moldado. Rio de Janeiro.
- [13] ASSOCIAÇÃO BRASILEIRA DE NORMAS TÉCNICAS. NBR 9062 (2006). NBR 9062: Projeto e execução de estruturas de concreto pré-moldado. Rio de Janeiro.
- [14] Recommended practice for the design of prestressed concrete columns and walls (1988). Journal of Prestressed Concrete Institute, Chicago, v.33, n. 4, p. 56-95.
- [15] CARVALHO, R. C.; FIGUEIREDO, J. R. (2004). Cálculo e detalhamento de estruturas usuais de concreto armado. São Carlos. EdUFSCar.
- [16] FRANÇA, R.L.S. (1991). Contribuição ao estudo dos efeitos de segunda ordem em pilares de concreto armado. 232f. Tese (Doutorado) - Escola Politécnica, Universidade de São Paulo, São Paulo, 1991.
- [17] ASSOCIAÇÃO BRASILEIRA DE NORMAS TÉCNICAS. NBR 8681 (2003). NBR 8681: Ações e segurança nas estruturas - Procedimento. Rio de Janeiro.
- [18] FÉDÉRATION INTERNACIONALE DU BETON (1999). Structural concrete: textbook on behavior on design and performance update of the CEB/FIP model code 1990. Bulletin FIB. Lausanne, v.1-3.
- [19] MARIN, M.C. (2009). Contribuição à análise da estabilidade global de estruturas em concreto pré-moldado de múltiplos pavimentos. 213f. Dissertação (Mestrado) - Escola de Engenharia de São Carlos, Universidade de São Paulo, São Carlos, 2009.
- [20] FUSCO, P.B. (1981). Estruturas de concreto: solicitações normais, estados limites, teoria e aplicações. Rio de Janeiro: Guanabara Dois.
- [21] OLIVEIRA, P.H.S. (2004). Processo aproximado para consideração da não-linearidade física de pilares em concreto armado. 208f. Dissertação (Mestrado) - Escola Politécnica, Universidade de São Paulo, São Paulo, 2004.
- [22] EL DEBS, M.K.; MIOTTO, A.M.; EL DEBS, A.L.H.C. (2010). Analysis of a semi-rigid connection for precast concrete. Buildings & Structures.
- [23] ASSOCIAÇÃO BRASILEIRA DE NORMAS TÉCNICAS. NBR 6123 (1988). NBR 6123: Forças devidas ao vento em edificações. Rio de Janeiro.
- [24] ELLIOTT, K. S. (1996). Multi-storey precast concrete framed structures. Oxford: Blackwell Science, 1996.